



Charging and discharging electrochemical supercapacitors in the presence of both parallel leakage process and electrochemical decomposition of solvent

Shuai Ban^a, Jiujuun Zhang^{a,*}, Lei Zhang^a, Ken Tsay^a, Datong Song^a, Xinfu Zou^b

^a National Research Council of Canada, Vancouver, BC, Canada V6T 1W5

^b Department of Applied Mathematics, University of Western Ontario, London, ON, Canada N6A 5B7

ARTICLE INFO

Article history:

Received 5 November 2012

Received in revised form

14 December 2012

Accepted 15 December 2012

Available online 22 December 2012

Keywords:

Electrochemical supercapacitor

Charge and discharge

Parallel leakage

Self-discharging

Solvent decomposition

ABSTRACT

Simple models for electrochemical supercapacitors are developed to describe the charge–discharge behaviors in the presence of both voltage-independent parallel leakage process and electrochemical decomposition of solvent. The models are validated by experimental data collected using a symmetric two-electrode test cell with carbon powder as the electrode layer material and stainless steel as the current collector.

© 2013 Published by Elsevier Ltd.

1. Introduction

Electrochemical supercapacitors (ESs) are considered important energy efficiency devices for rapid energy storage and delivery. Among the advantages of ESs are high power density, long lifecycle, high efficiency, wide range of operating temperatures, environmental friendliness, and safety. ESs also serves as a bridging function for the power/energy gap of traditional dielectric capacitors. These characteristics have made ESs very competitive for applications in electric hybrid vehicles, digital communication devices such as mobile phones, digital cameras, electrical tools, pulse laser technique, uninterruptible power supplies, and storage of the energy generated by solar cells [1–3]. Unfortunately, there are still some challenges, such as low energy density, high cost, and high self-discharge rate, which have limited wider applications of ESs [3,4].

In order to increase energy density, according to the energy density expression $E = 1/2CV^2$, where E is the ES's energy density, C is the specific capacitance, and V is the cell voltage, respectively, two major approaches have been taken. One is to increase the specific capacitance (C) of the electrode material [3–6], and the other is to increase the cell voltage (V) using solvents such as non-aqueous

and ionic liquid solutions which have wider electrode potential windows [4,7–9]. From the energy density equation mentioned above, it is obvious that increasing cell voltage to enhance energy density is more effective than increasing the specific capacitance because the voltage is squared in the formula. However, if the cell voltage is too high, the electrochemical decomposition of solvent may occur due to the limited electrode material stability and/or solvent's thermodynamic decomposition windows. This solvent electrochemical decomposition could produce gaseous products, leading to the pressure build-up inside the cell, causing safety concerns, and self-discharge [10–17]. Another challenge of supercapacitors is the parallel leakages, causing a fast self-discharge, reducing the shelf-life. The main contributors to the parallel leakages of the supercapacitors can be summarized into four processes [7]: (1) Faradaic reaction of electrolyte impurities; (2) parasitic redox reactions involving impurities (oxygen groups and metals); (3) non-uniformity of charge acceptance along the surface of electrode material pores; and (4) possible short-circuit of the anode and cathode from improperly sealed bipolar electrodes. Due to these parallel leakages, the shelf-life could be significantly reduced when compared to those of electrochemical batteries [7].

To better understand the effects of parallel leakage process and/or electrochemical decomposition of solvent on supercapacitors' performance, some experimental and theoretical studies have been carried out to investigate the charge and discharge behaviors [18–23]. Since the parallel leakage process and the solvent decomposition are mainly related to the electrochemical

* Corresponding author at: 4250 Wesbrook Mall, Vancouver, B.C. V6T 1W5, Canada. Tel.: +1 604 221 3087; fax: +1 604 221 3001.

E-mail address: jiujuun.zhang@nrc.gc.ca (J. Zhang).

Nomenclature

Symbol, Meaning

α_n	electron transfer coefficient in the rate determining step of negative electrode reaction
α_p	electron transfer coefficient in the rate determining step of positive electrode reaction
b_n	Tafel slope of the negative electrode reaction
b_p	Tafel slope of the positive electrode reaction
C	capacitance (F cm^{-2})
C_{dl}	double-layer capacitance (F cm^{-2})
C_m	specific capacitance (F g^{-1})
C_s	mole concentration of the solvent (mol cm^{-3})
ΔV^0	$= V_p^0 - V_n^0 - b_p \ln(i_p^0) - b_n \ln(i_n^0)$
e^-	electron
E	energy density (Wh cm^{-2})
$(E_m)_{\max}$	maximum energy density of the supercapacitor (Wh kg^{-1})
F	Faraday's constant ($96,487 \text{ C mol}^{-1}$)
i_F	current density induced by the solvent electrochemical decomposition (A cm^{-2})
i_n	current density of the negative electrode reaction (A cm^{-2})
i_p	current density of the positive electrode reaction (A cm^{-2})
i_{sc}	charging or discharging current density of the supercapacitor (A cm^{-2})
I_{cell}	constant current density for charging or discharging the supercapacitor (A cm^{-2})
k_n	reaction constant of the negative electrode reaction (cm s^{-1})
k_p	reaction constant of the positive electrode reaction (cm s^{-1})
m	mass of the electrode material (g)
$n_{\alpha n}$	electron transfer number in the rate determining step of negative electrode reaction
$n_{\alpha p}$	electron transfer number in the rate determining step of positive electrode reaction
n_n	overall electron transfer number in the negative electrode reaction
n_p	overall electron transfer number in the positive electrode reaction
p_n	product of the negative electrode reaction
p_p	product of the positive electrode reaction
$(P_m)_{\max}$	maximum power density of the supercapacitor (W kg^{-1})
R	universal gas constant ($8.314 \text{ J K}^{-1} \text{ mol}^{-1}$)
R_{esr}	equivalent series resistance of the supercapacitor ($\Omega \text{ cm}^2$)
R_{lk}	equivalent leakage resistance ($\Omega \text{ cm}^2$)
S	reactant of the solvent
t	time (s)
t_{fd}	time needed for a supercapacitor being fully discharged (s)
T	temperature (K)
T_s	time needed when the supercapacitor voltage goes down to 95% of its maximum voltage (s)
V	voltage (V)
V_{cell}	voltage of the supercapacitor cell (V)
V_{cell}^{\max}	maximum voltage of the supercapacitor cell (V)
V_F	voltage induced by the solvent electrochemical decomposition (V)
V_n	negative electrode potential of the solvent electrochemical decomposition (V)

V_n^0	standard electrode potentials for negative electrode reaction (V)
V_p	positive electrode potential of the solvent electrochemical decomposition (V)
V_p^0	standard electrode potentials for positive electrode reaction (V)
V_{sc}	supercapacitor voltage (V)
V_{sc}^{\max}	designed charging voltage of the supercapacitor (V)
V_{sc}^0	maximum supercapacitor voltage (V)

processes occurring inside the supercapacitor cells, describing the charge and discharge behaviors by electrochemical parameters, such as equivalent series resistance, capacitance, and several electrode kinetic constants, seems more appropriate, in particular for electrochemical decomposition of the solvent.

In this paper, for fundamental understanding of supercapacitor charging and discharging behaviors, through experiment validation we present some simple mathematical models incorporating the voltage-independent parallel leakage process and electrochemical decomposition to describe the supercapacitor charge and discharge behaviors. Using these models, the experiment data could be simulated to obtain the desired values of parameters such as specific capacitance and equivalent series resistance from which both the energy and power density can be calculated. The simulated parameter values related to both parallel leakages and solvent decomposition could be used to predict supercapacitor's self-discharge and shelf-life, performance/efficiency losses, as well as the limiting workable cell voltage of the supercapacitors. Therefore, the proposed models are useful in evaluating and diagnosing supercapacitor cells. We hope these simple models could be used as a tool for understanding the charging–discharging behavior of the supercapacitors. Furthermore, we believe that these models could also be useful in obtaining the essential parameters of the supercapacitors such as equivalent series resistance and capacitance based on the recorded curves of charging–discharging.

2. Experimental

2.1. Electrode layer preparation

For electrode layer materials, Carbon black BP2000 (Cabot Corporation), conducting carbon Super C45 (from TIMCAL), and 60 wt% Polytetrafluoroethylene (PTFE)–water dispersion (Aldrich) were used as received without further modification.

For electrode layer preparation, the procedure has been described in our previous publication [3], and is repeated as below. Carbon and conducting carbon powders were first mixed with a Vortex Mixer (Thermo Scientific) for 30 min to form a uniformly-mixed powder, which was then transferred into a beaker containing both PTFE binder and ethanol solution under constant stirring to form a suspension. After the solvent was evaporated at high temperature, the paste formed was collected on a glass slide. This paste was manipulated by repeatedly folding and pressing using a spatula until a sufficient mechanical strength was achieved. Then this paste was rolled to a thin electrode sheet with the required thickness using a MTI rolling press. Finally, this electrode sheet was placed into a vacuum oven at 90°C under active vacuum for at least 12 h. The formed dry electrode sheet was cut into two 2×2 square centimeters (cm^2) for electrode layers, which were then sandwiched with a $30 \mu\text{m}$ thick porous PTFE separator (W. L. Gore & Associates, Inc.) in the middle, forming an electrode separator assembly (ESA). The assembly was then impregnated with an aqueous electrolyte containing $0.5 \text{ M Na}_2\text{SO}_4$ inside a vacuum oven at 60°C for at least

one hour. This electrolyte-impregnated ESA was then assembled into the two-electrode test cell.

2.2. Two-electrode test cell measurements

In the two-electrode test cell [24], the active electrode surface for both positive and negative electrodes was 4.0 cm^2 . The electrolyte was $0.5 \text{ M Na}_2\text{SO}_4$ aqueous solution, and the current collectors were made of stainless steel. The additional effect of electrolyte concentration on supercapacitor's performance was carefully studied in our previous publication [24]. For electrochemical measurements, both cyclic voltammograms and galvanic charge–discharge curves were recorded using a Solartron 1287 potentiostat. For cell internal resistance measurements, AC impedance spectra at a frequency range of $0.1 \text{ Hz}–10 \text{ kHz}$ were collected using a Solartron FRA analyzer. For a more detailed description about the measurement and calculation procedures, please see our previous publication [24].

For recording charging/discharging curves of supercapacitors, there are mainly two options, one is to control a constant charging–discharging current, then record the change of cell voltage with time, and the other is to control a constant cell voltage, then record the change of cell current with time. The most popular option is the former. In this paper, we used the former option to obtain the charging–discharging curves.

All measurements were made at room temperature and ambient pressure.

3. Results and discussion

In general, for charging and discharging a supercapacitor, there are two major options. One is the charging or discharging at a constant cell voltage to record the cell current change with time, and the other is charging or discharging at a constant current to record that cell voltage change with time. In this paper, we will only focus on the charging and discharging at a constant current.

3.1. Charging at a constant cell current in the absence of parallel leakage process and electrochemical decomposition of solvent

Fig. 1(a) depicts a proposed equivalent circuit for a double-layer supercapacitor with a constant current in the absence of both voltage-independent parallel leakage process and electrochemical decomposition of the solvent, where K is the electric switcher, R_{esr} is the equivalent series resistance, I_{cell} is the constant current for charging or discharging the supercapacitor; V_{cell} is the supercapacitor cell voltage; C_{dl} is the double-layer capacitance; V_{sc} is the voltage across the C_{dl} ; and i_{sc} is the current used to charge or discharge, respectively. Note that in the case shown in Fig. 1(a), the current used to charge or discharge the double layer capacitance (i_{sc}) is equal to the charging current (I_{cell}), which has a constant value:

$$I_{cell} = i_{sc} \quad (1)$$

assuming that, before the charging starts, the supercapacitor is at zero-charge state, that is, the voltage across the supercapacitor (V_{sc}) is equal to zero. When the switch is turned on at $t=0$ (t is the charging time), the charge process is then started and the voltage across the supercapacitor can be expressed as:

$$V_{sc} = \frac{1}{C_{dl}} \int_{t=0}^{t=t} i_{sc} dt = \frac{1}{C_{dl}} \int_{t=0}^{t=t} I_{cell} dt = \frac{I_{cell}}{C_{dl}} t \quad (2)$$

therefore, the supercapacitor cell voltage can be expressed as:

$$V_{cell} = I_{cell}R_{esr} + V_{sc} = I_{cell}R_{esr} + \frac{I_{cell}}{C_{dl}} t \quad (\text{charge process}) \quad (3)$$

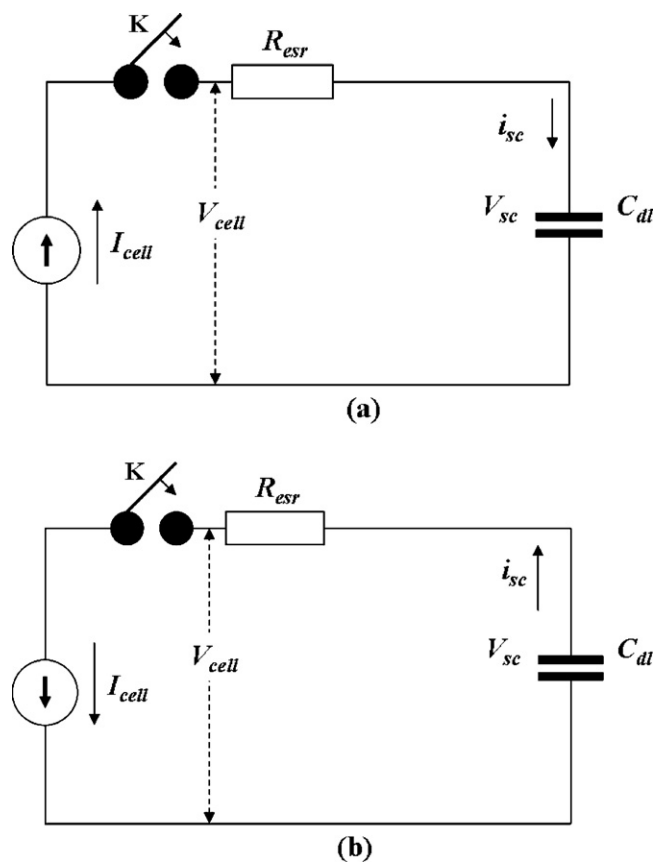


Fig. 1. Proposed equivalent circuits of a double-layer supercapacitor at a constant current charging (a) and discharging (b) in the absence of both parallel leakage process and electrochemical decomposition of the solvent. K : electric switcher; R_{esr} : equivalent series resistance; I_{cell} : constant current for charging or discharging the supercapacitor; V_{cell} : supercapacitor cell voltage; C_{dl} : double-layer capacitance; V_{sc} : voltage across the C_{dl} ; and i_{sc} : current used to charge or discharge C_{dl} , respectively.

Eq. (3) suggests that the cell voltage is linearly proportional to the charge time. If the supercapacitor is charged to a designed cell voltage of V_{cell}^{max} , a discharge process at a constant current (I_{cell}) can be started immediately, as shown in Fig. 1(b). Note that at this desired cell voltage (or maximum cell voltage) of V_{cell}^{max} , the voltage across the double layer capacitance (C_{dl}), V_{sc}^o , should be given by:

$$V_{sc}^o = V_{cell}^{max} - I_{cell}R_{esr} \quad (4)$$

in the case of discharging, this V_{sc}^o will be the load to discharge the supercapacitor. The cell voltage (V_{cell}) can be expressed by the following equation

$$V_{cell} = V_{sc}^o - I_{cell}R_{esr} - \frac{I_{cell}}{C_{dl}} t \quad (\text{discharge process}) \quad (5)$$

As an example, Fig. 2 shows the charge–discharge curves using a two-electrode test cell in which two electrodes are identical (symmetric cell). Based on both Eqs. (3) and (5), several parameters such as the double-layer capacitance (C_{dl}), the voltage across the double layer capacitance at the end of charging (V_{sc}^o), as well as equivalent series resistance (R_{esr}) can be simulated, respectively, using both the charge and discharge curves. In the case shown in Fig. 2, parameters obtained using the simulation are: capacitance $C_{dl} = 0.127 \text{ F cm}^{-2}$ or 0.509 F for the entire cell with electrode area of 4 cm^2 , or the specific capacitance (C_m) of 34 F g^{-1} for the carbon loading (m) of 0.015 g for each electrode; the voltage across the double layer capacitance $V_{sc}^o = 0.991 \text{ V}$; as well as the equivalent series resistance $R_{esr} = 2.36 \text{ } \Omega \text{ cm}^2$ or $0.589 \text{ } \Omega$ for the entire cell, respectively. Note that the specific capacitance obtained here was also

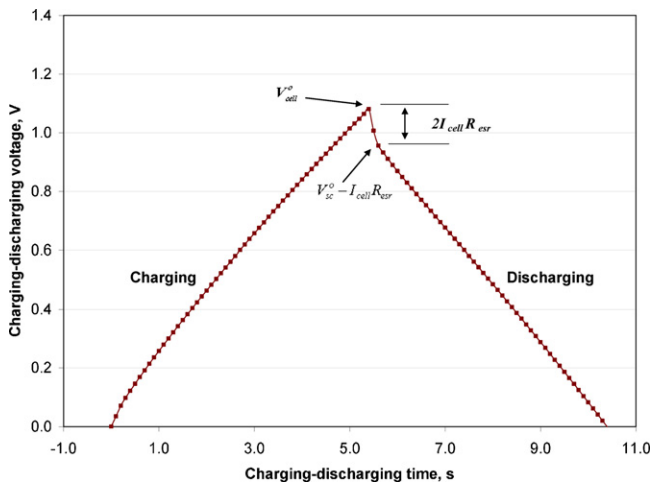


Fig. 2. Charge–discharge curves recorded using a symmetric supercapacitor cell with a geometric area of 4.0 cm^2 for each electrode, in $0.5 \text{ M Na}_2\text{SO}_4$ aqueous solution at ambient conditions. Stainless steel sheets as both the positive and negative current collectors. Charge and discharge current density: 0.025 A cm^{-2} , and total BP 2000 carbon loading of electrode layers: 3.8 mg cm^{-2} . Note that the R_{esr} showing in the figure should be the sum equivalent series resistances of both positive and negative electrodes [24]. Note that the curve corresponds to the simulation and the points to experimental data.

confirmed by using cyclic voltammetry measurements. Using these values, the maximum energy and power densities ($(E_m)_{\max}$ and $(P_m)_{\max}$, respectively) can be calculated according to the equations presented in our previous publication [24]: $(E_m)_{\max} = 1/2 C_m (V_{sc}^o)^2$, and $(P_m)_{\max} = 1/4 m ((V_{sc}^o)^2 / R_{esr})$. The obtained $(E_m)_{\max}$ and $(P_m)_{\max}$ are 4.64 Wh kg^{-1} , and $2.78 \times 10^4 \text{ Wh kg}^{-1}$, respectively.

3.2. Charging at a constant cell current in the presence of a voltage-independent parallel leakage process

Fig. 3 shows the scheme of a supercapacitor charging at a constant current density. Compared to Fig. 1, there is an additional equivalent leakage resistance (R_{lk}) which represents a voltage-independent parallel leakage process. Note that for simplicity, we treat all voltage-insensitive leakage processes as an equivalent parallel leakage (R_{lk}), suggesting that the magnitude of this R_{lk} would not significantly change with the charge or discharge process. However, we do need to keep it in mind that this R_{lk} may change with cell voltage in practice.

Again, we assume that before the charge process starts, the supercapacitor is at zero-charge state, that is, the voltage across the supercapacitor is equal to zero. When the switch shown in Fig. 3(a) is closed at $t=0$, the charge process is started. When $t \geq 0$, the supercapacitor charging voltage can be expressed by

$$C_{dl} \frac{dV_{sc}}{dt} + \frac{V_{sc}}{R_{lk}} - I_{cell} = 0 \quad (6)$$

solving Eq. (6) with the initial condition $t=0$, $V_{sc}=0$, the following solution can be obtained:

$$V_{sc} = I_{cell} R_{lk} \left(1 - \exp\left(-\frac{t}{R_{lk} C_{dl}}\right) \right) \quad (\text{charge process}) \quad (7)$$

accordingly the cell voltage can be expressed as:

$$V_{cell} = I_{cell} R_{esr} + I_{cell} R_{lk} \left(1 - \exp\left(-\frac{t}{R_{lk} C_{dl}}\right) \right) \quad (\text{charge process}) \quad (8)$$

Eq. (8) shows that at $t=0$, $V_{cell}=I_{cell}R_{esr}$, and when $t=\infty$, $V_{cell}=I_{cell}R_{esr}+I_{cell}R_{lk}$. In this case, the voltage across the supercapacitor (V_{sc}) increasingly approaches its maximum value, defined

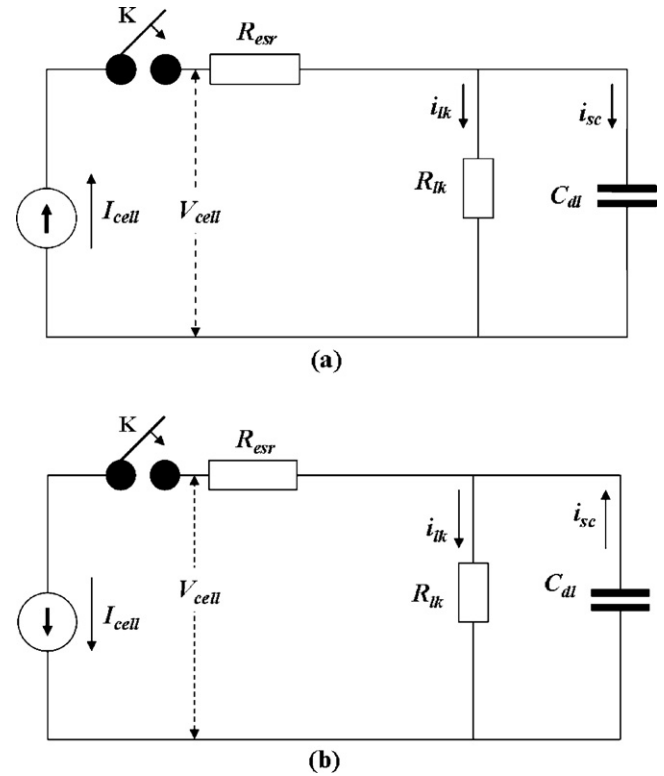


Fig. 3. Proposed equivalent circuits of a double-layer supercapacitor by constant current charging (a) and discharging (b) in the presence of parallel leakage process. K: electric switch; R_{lk} : equivalent parallel leakage resistance; R_{esr} : equivalent series resistance; I_{cell} : constant current for charging or discharging the supercapacitor; V_{cell} : supercapacitor cell voltage; C_{dl} : double-layer capacitance; V_{sc} : voltage across the C_{dl} ; and i_{sc} : current used to charge or discharge C_{dl} , respectively.

as V_{sc}^o which is equal to $I_{cell}R_{lk}$ as t tends to infinity. If there is no leakage current, $R_{lk} \rightarrow \infty$, for small t , Eq. (8) can be approximated by

$$V_{cell} = I_{cell} R_{esr} + I_{cell} \frac{t}{C_{dl}} \quad (\text{charge process}) \quad (9)$$

note that if charging an ideal supercapacitor ($R_{esr}=0$, and $R_{lk}=\infty$) using a constant current, the cell voltage will become:

$$V_{cell} = I_{cell} \frac{t}{C_{dl}} \quad (10)$$

In a later section, we will give a detailed discussion about the effect of solvent electrochemical decomposition on the supercapacitor charge and discharge behaviors.

After the supercapacitor cell is fully charged with a maximum voltage of (V_{sc}^o), a discharge process using a constant current (I_{cell}) will be started for which the equivalent circuit can be illustrated in Fig. 3(b). The integration equation used to describe this situation is:

$$\frac{1}{C_{dl}} \int_{t=0}^{t=t} i_{sc} dt + i_{sc} R_{lk} - (V_{sc}^o + I_{cell} R_{lk}) = 0 \quad (11)$$

solving this equation, we can get:

$$i_{sc} = \frac{(V_{sc}^o + I_{cell} R_{lk})}{R_{lk}} \exp\left(-\frac{t}{R_{lk} C_{dl}}\right) \quad (12)$$

and the voltage across the double-layer capacitance can be expressed as:

$$\begin{aligned} V_{sc} &= V_{sc}^o - \frac{1}{C_{dl}} \int_{t=0}^{t=t} i_{sc} dt \\ &= V_{sc}^o - (V_{sc}^o + I_{cell} R_{lk}) \left[1 - \exp\left(-\frac{t}{R_{lk} C_{dl}}\right) \right] \end{aligned} \quad (13)$$

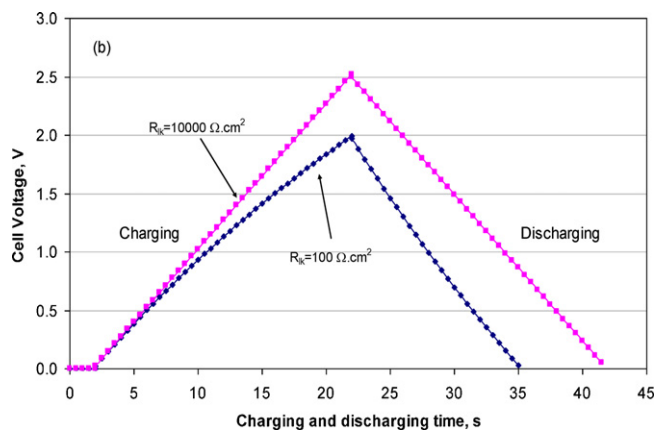


Fig. 4. Theoretically calculated charge–discharge curves, R_{lk} is changed from 100 to 10,000 $\Omega \text{ cm}^2$ with fixed $R_{esr} = 0.5 \Omega \text{ cm}^2$, $C_{dl}^T = 0.4 \text{ F/cm}^2$, and $I_{cell} = 0.05 \text{ A/cm}^2$.

the cell voltage (V_{cell}) can be expressed by:

$$V_{cell} = -I_{cell}R_{esr} + V_{sc}^o - (V_{sc}^o + I_{cell}R_{lk}) \times \left[1 - \exp\left(-\frac{t}{R_{lk}C_{dl}}\right) \right] \quad (\text{discharge process}) \quad (14)$$

if there is no parallel leakage process ($R_{lk} \rightarrow \infty$), for limited t , Eq. (14) can be approximated by

$$V_{cell} = -I_{cell}R_{esr} + V_{sc}^o - I_{cell} \frac{t}{C_{dl}} \quad (15)$$

the supercapacitor full discharge time, denoted by t_{fd} , can be derived by setting $V_{sc} = 0$ and solving this equation for t , giving

$$t_{fd} = -R_{lk}C_{dl} \ln\left(\frac{I_{cell}R_{lk}}{V_{sc}^o + I_{cell}R_{lk}}\right) \quad (16)$$

As an example, Fig. 4 shows the theoretically calculated charge and discharge curves according to Eqs. (8) and (14). It can be seen that when the parallel leakage resistance becomes smaller (larger leakage current) from 10,000 to 100 $\Omega \text{ cm}^2$, both the cell voltage and the maximum supercapacitor voltage become smaller, suggesting that the performance of the supercapacitor cell is reduced.

Furthermore, due to the parallel leakage process, self-discharge will become significant. For example, if a fully charged supercapacitor with a voltage of V_{sc}^o is put on the shelf ($I_{cell} = 0$ in this case), according to Eq. (13), the voltage will be gradually reduced due to the self-discharge through R_{lk} . When the V_{sc} goes down to 95% of V_{sc}^{\max} , the time (T_s) for V_{sc} to reach this level is given by:

$$T_s = 2.996R_{lk}C_{dl} \quad (17)$$

in the situation of even $R_{lk} = 10,000 \Omega \text{ cm}^2$, and $C_{lk} = 0.4 \text{ F cm}^{-2}$, $T_s = 3.33 \text{ h}$. Therefore, self-discharge is one of the major challenges for supercapacitors.

3.3. Charging at a constant cell current in the presence of electrochemical decomposition of solvent

Fig. 5(a) shows the proposed equivalent circuit for a double-layer supercapacitor in the case of constant current charging in the presence of electrochemical decomposition of the solvent. Compared to Fig. 1, there is an additional parallel electrochemical process included with a potential dependent current (i_F) and voltage (V_F) induced by the solvent electrochemical decomposition. From the equivalent circuits in Fig. 5, it can be seen that $V_{sc} = V_F$.

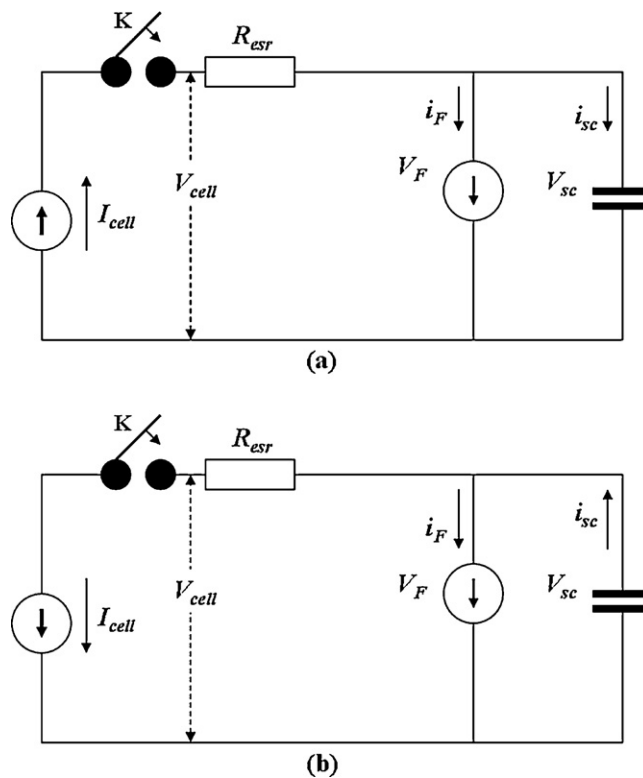


Fig. 5. Proposed equivalent circuits for a double-layer supercapacitor at a constant current charging (a) and discharging (b) in the presence of electrochemical decomposition of the solvent. K: electric switcher; R_{esr} : equivalent series resistance; I_{cell} : constant current for charging or discharging; V_{cell} : supercapacitor cell voltage; i_F : current of solvent electrochemical decomposition; C_{dl} : double-layer capacitance; i_{sc} : current used to charge or discharge the double-layer capacitance; V_F : electrode potential of the solvent electrochemical decomposition; and $V_{sc}(=V_F)$: voltage across the double-layer capacitance, respectively.

Assuming that the solvent (S) decomposition reactions at the positive and negative electrodes are expressed by the following Reactions (I) and (II), respectively:



here n_p is the overall electron number of S oxidation to produce P_p , and n_n is the overall electron number of S reduction to produce P_n , respectively. Assuming that both reactions are irreversible, the current density for Reaction (I) (i_p) and that for Reaction (II) (i_n) can be expressed by Eqs. (18) and (19), respectively:

$$i_p = n_p F k_p C_S \exp\left(\frac{\alpha_p n_{\alpha p} F (V_p - V_p^o)}{RT}\right) = i_p^o \exp\left(\frac{V_p - V_p^o}{b_p}\right) \quad (18)$$

$$i_n = n_n F k_n C_S \exp\left(\frac{\alpha_n n_{\alpha n} F (V_n^o - V_n)}{RT}\right) = i_n^o \exp\left(\frac{V_n^o - V_n}{b_n}\right) \quad (19)$$

Here $i_p^o = n_p F k_p C_S$ and $i_n^o = n_n F k_n C_S$ can be defined as the standard current densities, $b_p = RT/\alpha_p n_{\alpha p} F$ and $b_n = RT/\alpha_n n_{\alpha n} F$ can be defined as the Tafel slopes for Reactions (I) and (II); k_p and k_n are the reaction constants, α_p and α_n are the charge transfer coefficients, $n_{\alpha p}$ and $n_{\alpha n}$ are the electron transfer numbers in the reaction determining steps, V_p^o and V_n^o are the standard electrode potentials for Reactions (I) and (II); V_p and V_n are the electrode potential of the positive and negative electrodes, respectively. C_S is the mole concentration; F is Faraday's constant; R is the universal gas constant; and T is the temperature; respectively.

Note that because both Reactions (I) and (II) represent the solvent decomposition, the solvent concentration should not

be changed with its consumption by electrochemical reactions. Therefore, there is no mass transfer limitation involved in the electrochemical reactions.

From Eqs. (18) and (19), their electrode potentials can be derived as Eqs. (20) and (21), respectively:

$$V_p = V_p^o - b_p \ln(i_p^o) + b_p \ln(i_p) \quad (20)$$

$$V_n = V_n^o + b_n \ln(i_n^o) - b_n \ln(i_n) \quad (21)$$

from Fig. 5, it can be seen that the voltage drop across the double-layer capacitance (V_{sc}) can be expressed as:

$$V_{sc} = V_p - V_n = V_p^o - V_n^o - b_p \ln(i_p^o) - b_n \ln(i_n^o) + b_p \ln(i_p) + b_n \ln(i_n) \quad (22)$$

$$= \Delta V^o + b_p \ln(i_p) + b_n \ln(i_n)$$

where

$$\Delta V^o = V_p^o - V_n^o - b_p \ln(i_p^o) - b_n \ln(i_n^o) \quad (23)$$

for a decomposition reaction, $i_p = i_n$, they should also be equal to i_F , as is shown in Fig. 5, that is, $i_F = i_p = i_n$. Substituting this into Eq. (22), the following equation for i_F can be obtained:

$$i_F = \exp\left(\frac{V_{sc} - \Delta V^o}{b_p + b_n}\right) \quad (24)$$

In the case of constant current charging as shown in Fig. 5, we assume that before the charging starts, the voltage across the supercapacitor (V_{sc}) is equal to zero. Then the charging current (i_{sc}) used to charging double-layer capacitance (C_{dl}) can be expressed as:

$$i_{sc} = C_{dl} \frac{dV_{sc}}{dt} \quad (25)$$

in Fig. 5(a), the constant charging current can be expressed as:

$$I_{cell} = i_{sc} + i_F \quad (26)$$

Using Eq. (28), the maximum voltage (V_{sc}^o) across the double-layer capacitance can also be derived by setting $t \rightarrow \infty$ (the moment when the supercapacitor is fully charged):

$$V_{sc}^o = (b_p + b_n) \ln\left(I_{cell} \exp\left(\frac{\Delta V^o}{b_p + b_n}\right)\right) \quad (30)$$

The maximum supercapacitor cell charging voltage (V_{cell}^{\max}) can be expressed as the sum of the voltage drop across the equivalent series resistance (R_{esr}) and the maximum voltage across the double-layer capacitance (V_{sc}^o):

$$\begin{aligned} V_{cell}^{\max} &= I_{cell} R_{esr} + V_{sc}^o \\ &= I_{cell} R_{esr} + (b_p + b_n) \ln\left(I_{cell} \exp\left(\frac{\Delta V^o}{b_p + b_n}\right)\right) \end{aligned} \quad (31)$$

for example, if the solvent is water, one has $V_p^o = 1.23V$ and $V_n^o = 0.00V$ vs. NHE. Assuming that the kinetic parameters $b_p = b_n = 0.0514V/\text{dec.}$, $i_p = 1.0 \times 10^{-7} \text{ A cm}^{-2}$, $i_n = 1.0 \times 10^{-3} \text{ A cm}^{-2}$ for water decomposition ($\text{H}_2\text{O} \rightarrow \frac{1}{2}\text{O}_2^{\uparrow} + 2\text{H}^+ + 2\text{e}^-$), and $C_{dl} = 0.125 \text{ F cm}^{-2}$, V_{sc}^o can then be calculated to be 2.034V at a charging current density of 0.025 A cm^{-2} .

For the discharge case shown in Fig. 5(b), the integration equation can be written as:

$$\frac{1}{(b_p + b_n)C_{dl}} \int_{t=0}^{t=t} i_{sc} dt + \ln(i_{sc} - I_{cell}) - \left(\frac{V_{sc}^o - \Delta V^o}{b_p + b_n}\right) = 0 \quad (32)$$

Solving this equation, we can get i_{sc} from which the voltage across the double layer capacitance (V_{sc}) can be derived respectively:

$$i_{sc} = \frac{I_{cell}(\exp(V_{sc}^o - \Delta V^o/b_p + b_n) + I_{cell})}{I_{cell} + \exp(V_{sc}^o - \Delta V^o/b_p + b_n)(1 - \exp(-(I_{cell}/(b_p + b_n)C_{dl}))t)} \quad (33)$$

$$V_{sc} = V_{sc}^o - (b_p + b_n) \ln\left[\frac{(\exp(V_{sc}^o - \Delta V^o/b_p + b_n) + I_{cell}) \exp(I_{cell}/(b_p + b_n)C_{dl})t - \exp(V_{sc}^o - \Delta V^o/b_p + b_n)}{I_{cell}}\right] \quad (34)$$

Eq. (34) indicates that when $t=0$, $V_{sc} = V_{sc}^o$. The supercapacitor cell charging voltage (V_{cell}) can be expressed as:

$$\begin{aligned} V_{cell} &= -I_{cell} R_{esr} + V_{sc} \\ &= -I_{cell} R_{esr} + V_{sc}^o - (b_p + b_n) \ln\left[\frac{(\exp(V_{sc}^o - \Delta V^o/b_p + b_n) + I_{cell}) \exp(I_{cell}/(b_p + b_n)C_{dl})t - \exp(V_{sc}^o - \Delta V^o/b_p + b_n)}{I_{cell}}\right] \end{aligned} \quad (\text{discharge process}) \quad (35)$$

Combining Eqs. (24), (25) and (26), the following differential equation can be obtained:

$$C_{dl} \frac{dV_{sc}}{dt} + \exp\left(\frac{-\Delta V^o}{b_p + b_n}\right) \exp\left(\frac{V_{sc}}{b_p + b_n}\right) - I_{cell} = 0 \quad (27)$$

With the initial condition $V_{sc} = 0$ at $t = 0$, Eq. (27) can be solved to obtain:

$$V_{sc} = (b_p + b_n) \ln\left(\frac{I_{cell}}{I_{cell} - \exp(-\Delta V^o/b_p + b_n)) \exp(-I_{cell}/(b_p + b_n)C_{dl}t) + \exp(-\Delta V^o/b_p + b_n)}\right) \quad (\text{charge process}) \quad (28)$$

The supercapacitor cell charging voltage (V_{cell}) should be the sum of the voltage drop across the equivalent series resistance (R_{esr}) and the voltage across the double-layer capacitance (V_{sc}):

$$\begin{aligned} V_{cell} &= I_{cell} R_{esr} + V_{sc} \\ &= I_{cell} R_{esr} + (b_p + b_n) \ln\left(\frac{I_{cell}}{I_{cell} - \exp(-\Delta V^o/b_p + b_n)) \exp(-I_{cell}/(b_p + b_n)C_{dl}t) + \exp(-\Delta V^o/b_p + b_n)}\right) \end{aligned} \quad (\text{charge process}) \quad (29)$$

As an illustration, Fig. 6 shows the charge and discharge curves calculated according to Eqs. (29) and (35). It can be seen that the solvent decomposition plateau voltages (ΔV^o Eq. (23)) are all higher than the thermodynamic voltages because of the limited kinetic processes. However, for a safe operation of supercapacitor, it is better not to charge the cell to a thermodynamic voltage of solvent decomposition. For example, if using water as the solvent, the maximum charging voltage should not be higher than 1.23V.

It is worthwhile to point out that the model shown in Fig. 5(a) and its associated equations discussed above do not include the reactant mass transfer limitation since there may not be a limited

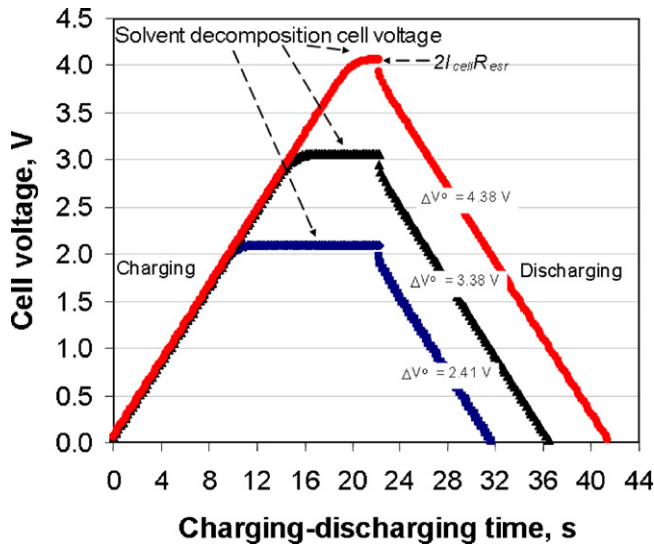


Fig. 6. Calculated charge–discharge curves according to Eqs. (29) and (35) using the following assumed parameters: $b_p = b_n = 0.0514 \text{ V/dec.}$, $i_p = 1.0 \times 10^{-7} \text{ A cm}^{-2}$, $i_n = 1.0 \times 10^{-3} \text{ A cm}^{-2}$, $C_{dl} = 0.125 \text{ F cm}^{-2}$, and $I_{cell} = 0.025 \text{ A cm}^{-2}$ at three different thermodynamic cell voltages ($V_p - V_n$) (1.23, 2.20, and 3.20 V, respectively).

supply of reactants. However, please also note that the build of product gasses in a closed cell, such as O_2 and H_2 if using an aqueous electrolyte, may lead to mass transport limitations and also pressure building-up, which will have some impact on the accuracy of the model.

3.4. Charging at a constant cell current in the presence of both voltage-independent parallel leakage process and electrochemical decomposition of solvent

Fig. 7(a) shows the proposed equivalent circuit of a double-layer supercapacitor in the case of constant current charging in the presence of both parallel leakage process and electrochemical decomposition of the solvent. The integration equation at a constant charging current (I_{cell}) can be written as:

$$i_{sc} + \exp\left(\frac{-\Delta V^o}{b_p + b_n}\right) \exp\left(\frac{1}{(b_p + b_n)C_{dl}} \int_{t=0}^{t=t} i_{sc} dt\right) + \frac{1}{R_{lk}C_{dl}} \int_{t=0}^{t=t} i_{sc} dt - I_{cell} = 0 \quad (36)$$

and for the discharge process at a constant current (I_{cell}):

$$i_{sc} - \exp\left(\frac{V_{sc}^o - \Delta V^o}{b_p + b_n}\right) \exp\left(-\frac{1}{(b_p + b_n)C_{dl}} \int_{t=0}^{t=t} i_{sc} dt\right) - \frac{1}{R_{lk}C_{dl}} \int_{t=0}^{t=t} i_{sc} dt - I_{cell} = 0 \quad (37)$$

Unfortunately, both of these two equations cannot be solved analytically, and numeric solutions will be sought using the software Matlab.

Fig. 8 shows the numeric solutions for both charge and discharge curves with several sets of assumed parameters in the presence of both voltage-independent parallel leakage resistance and solvent decomposition. The cell voltage (V_{cell}) for the charge process in this figure is expressed as:

$$V_{cell} = I_{cell}R_{esr} + V_{sc} = I_{cell}R_{esr} + \frac{1}{C_{dl}} \int_{t=0}^{t=t} i_{sc} dt \quad (38)$$

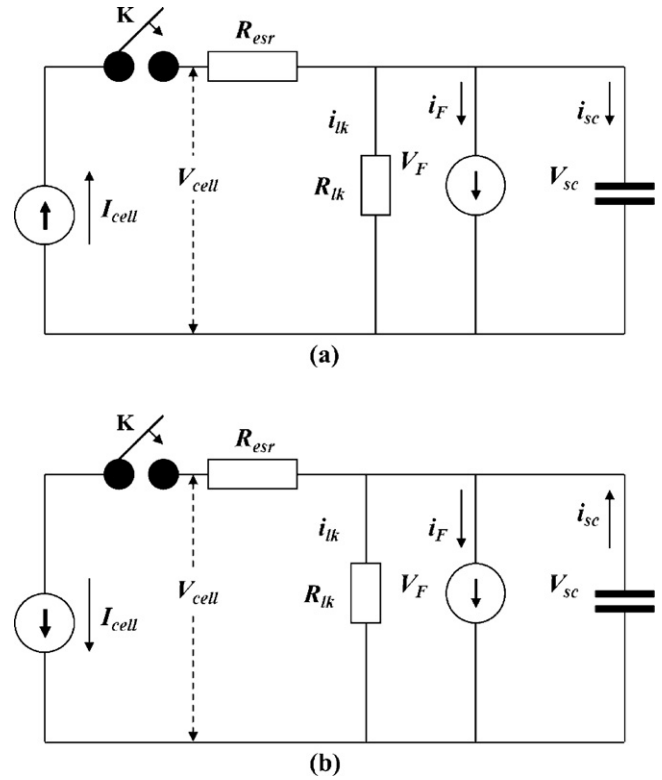


Fig. 7. Proposed equivalent circuits for a double-layer supercapacitor at a constant current charging (a) and discharging (b) in the presence of electrochemical decomposition of the solvent. K: electric switcher; R_{esr} : equivalent series resistance; R_{lk} : parallel leakage resistance; i_{lk} : parallel leakage current; I_{cell} : constant current for charging or discharging; V_{cell} : supercapacitor cell voltage; i_f : current of solvent electrochemical decomposition; C_{dl} : double-layer capacitance; i_{sc} : current used to charge or discharge the double-layer capacitance; and $V_{sc}(=V_F)$: voltage across the double-layer capacitance, respectively.

For the discharge process, the cell voltage in this figure is expressed as:

$$V_{cell} = -I_{cell}R_{esr} + V_{sc} = -I_{cell}R_{esr} + V_{sc}^o - \frac{1}{C_{dl}} \int_{t=0}^{t=t} i_{sc} dt \quad (39)$$

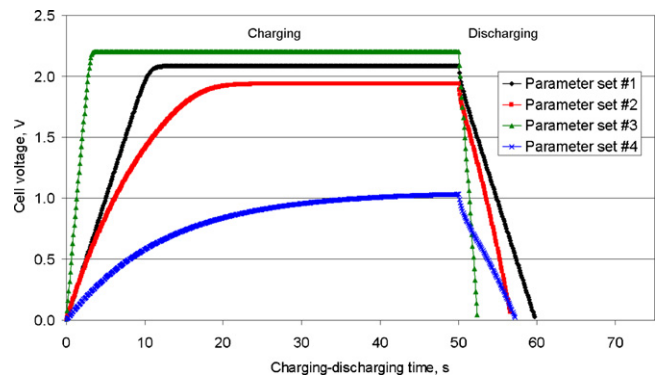


Fig. 8. Charge–discharge curves plotted by numeric solutions of Eqs. (36)–(39) using the following assumed parameter sets: set #1 $b_p = b_n = 0.0514 \text{ V/dec.}$, $\Delta V^o = 2.413 \text{ V}$, $R_{lk} = 10,000 \Omega \text{ cm}^2$, $C_{dl} = 0.125 \text{ F cm}^{-2}$, and $I_{cell} = 0.025 \text{ A cm}^{-2}$, $V_{sc}^{\text{max}} = 2.034 \text{ V}$, $R_{esr} = 2 \Omega \text{ cm}^2$; set #2 $b_p = b_n = 0.0514 \text{ V/dec.}$, $\Delta V^o = 2.413 \text{ V}$, $R_{lk} = 100 \Omega \text{ cm}^2$, $C_{dl} = 0.125 \text{ F cm}^{-2}$, and $I_{cell} = 0.025 \text{ A cm}^{-2}$, $V_{sc}^{\text{max}} = 2.034 \text{ V}$, $R_{esr} = 2 \Omega \text{ cm}^2$; set #3 $b_p = b_n = 0.0514 \text{ V/dec.}$, $\Delta V^o = 2.413 \text{ V}$, $R_{lk} = 100 \Omega \text{ cm}^2$, $C_{dl} = 0.125 \text{ F cm}^{-2}$, and $I_{cell} = 0.1 \text{ A cm}^{-2}$, $V_{sc}^{\text{max}} = 2.034 \text{ V}$, $R_{esr} = 2 \Omega \text{ cm}^2$; set #4 $b_p = b_n = 0.0514 \text{ V/dec.}$, $\Delta V^o = 2.413 \text{ V}$, $R_{lk} = 100 \Omega \text{ cm}^2$, $C_{dl} = 0.125 \text{ F cm}^{-2}$, and $I_{cell} = 0.01 \text{ A cm}^{-2}$, $V_{sc}^{\text{max}} = 2.034 \text{ V}$, $R_{esr} = 2 \Omega \text{ cm}^2$, respectively.

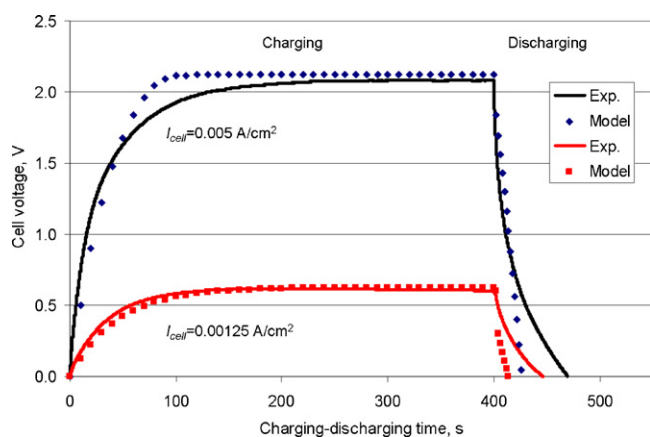


Fig. 9. Model fitting of Galvanic Cycledata with the measured parameters: $C_{dl} = 0.1 \text{ F cm}^{-2}$, (a) $I_{cell} = 0.0025 \text{ A cm}^{-2}$ and (b) $I_{cell} = 0.00125 \text{ A cm}^{-2}$ $R_{esr} = 0.55 \Omega \text{ cm}^2$. The fitting parameters are $b_p = b_n = 0.065 \text{ V/dec.}$, $\Delta V^0 = 2.413 \text{ V}$, $R_{ik} = 500 \Omega \text{ cm}^2$, and, $V_{sc}^{max} = 2.034 \text{ V}$.

To validate the models, the measured charge–discharge data at two different current densities are shown in Fig. 9 together with those simulated curves according to Eqs. (36)–(39). It can be seen that the model is reasonably fitting the experiment data, suggesting that the model developed in this paper can be used to describe the charge and discharge behaviors of electrochemical supercapacitors in the presence of both voltage-independent parallel leakage process and solvent decomposition. However, there is a slightly mismatching, in particular at the discharge curves. The difference between modeling and experiments could be originated from experimental trivial factors including the effect of gaseous evolution, dissolution of current collectors, electrolyte crystallization in separator, assembly quality, and so on. More work is definitely needed to take care of these affecting factors.

4. Conclusions

Mathematical models for electrochemical supercapacitors are developed to describe the charge–discharge behaviors in the presence of voltage-independent parallel leakage process and electrochemical decomposition of solvent. Four charge–discharge cases are discussed: (1) an ideal double-layer supercapacitor, (2) a supercapacitor in the presence of a voltage-independent parallel leakage process, (3) a supercapacitor in the presence of an electrochemical decomposition of solvent, and (4) a supercapacitor in the presence of both voltage-independent parallel leakage process and electrochemical decomposition of solvent. To validate these models, a symmetric two-electrode test cell with carbon powder as the electrode layer material and stainless steel as the current collector was assembled and used for charge–discharge data collection. A comparison of the simulation results based on the models and the experimental data seems to conclude that these models are valid in describing the charge and discharge behaviors of the supercapacitors. The analytical results are also helpful in identifying possible concerns of supercapacitors. For example, we have seen in Section 3.3 that the model predicts that self-discharge would be a major challenge for supercapacitor.

Acknowledgements

The authors would like to thank the support from National Research Council of Canada (NRC) and Transport Canada. Technical support from and discussion with Dr. Lucie Robitalille, Dr. Alexis Laforgue, Dr. Dongfang Yang, Dr. Yves Grincourt, Mr. Francois Girard, and Mr. Ryan Baker are highly appreciated.

References

- [1] F. Béguin, E. Raymundo-Piñero, Carbons for Electrochemical Energy Storage and Conversion Systems, CRC Press, Boca Raton, FL, 2010.
- [2] R. Kötz, M. Carlen, Principles and applications of electrochemical capacitors, *Electrochimica Acta* 45 (2000) 2483.
- [3] G. Wang, L. Zhang, J. Zhang, A review of electrode materials for electrochemical supercapacitors, *Chemical Society Reviews* 41 (2012) 797.
- [4] B.W. Ricketts, Self-discharge of carbon-based supercapacitors with organic electrolytes, *Journal of Power Sources* 89 (2000) 64.
- [5] C. Largeot, C. Portet, J. Chmiola, P. Taberna, Y. Gogotsi, P. Simon, Supercapacitors based on flexible graphene/polyaniline nanofiber composite films, *Journal of the American Chemical Society* 130 (2008) 2730.
- [6] J.S. Huang, B.G. Sumpter, V. Meunier, Theoretical model for nanoporous carbon supercapacitors, *Angewandte Chemie International Edition* 47 (2008) 520.
- [7] B.E. Conway, *Electrochemical Supercapacitors, Scientific Fundamentals and Technological Applications*, Kluwer Academic/Plenum Publishing, New York, 1999.
- [8] A. Lewandowski, A. Olejniczak, M. Galinski, I. Stepniak, Performance of carbon–carbon supercapacitors based on organic, aqueous and ionic liquid electrolytes, *Journal of Power Sources* 195 (2010) 5814.
- [9] A. Lewandowski, M. Galinski, Practical and theoretical limits for electrochemical double-layer capacitors, *Journal of Power Sources* 173 (2007) 822.
- [10] H. Zhao, Y. Zhang, Self-discharge analysis and characterization of supercapacitors for environmentally powered wireless sensor network applications, *Journal of Power Sources* 196 (2011) 8866.
- [11] K. Chiba, T. Ueda, Y. Yamaguchi, Y. Oki, F. Shimodate, K. Naoi, Electrolyte systems for high withstand voltage and durability I. linear sulfones for electric double-layer capacitors, *Journal of the Electrochemical Society* 158 (2011) A872.
- [12] P. Kurzweil, M. Chwisetek, Electrochemical stability of organic electrolytes in supercapacitors: spectroscopy and gas analysis of decomposition products, *Journal of Power Sources* 176 (2008) 555.
- [13] A.M. Bittner, M. Zhu, Y. Yang, H.F. Waibel, M. Knouma, U. Starke, C.J. Weber, Ageing of electrochemical double layer capacitors, *Journal of Power Sources* 203 (2012) 262.
- [14] I. Nicotera, G.D. McLachlan, G.D. Bennett, I. Plitz, F. Badway, G.G. Amatucci, S.G. Greenbaum, Solid-state NMR characterization of electrolyte breakdown products in nonaqueous asymmetric hybrid supercapacitors, *Electrochemical and Solid-State Letters* 10 (2007) A5.
- [15] T. Abdallah, D. Lemordant, B. Claude-Montigny, Are room temperature ionic liquids able to improve the safety of supercapacitors organic electrolytes without degrading the performances? *Journal of Power Sources* 201 (2012) 353.
- [16] R. Kotz, M. Hahn, P. Ruch, R. Gally, Comparison of pressure evolution in supercapacitor devices using different aprotic solvents, *Electrochemistry Communications* 10 (2008) 359.
- [17] S. Ishimoto, Y. Asakawa, M. Shinya, K. Naoi, Degradation responses of activated-carbon-based EDLCs for higher voltage operation and their factors, *Journal of the Electrochemical Society* 156 (2009) A563.
- [18] E. Tironi, V. Musolino, Supercapacitor characterization in power electronic applications: proposal of a new model, 2009 International Conference on Clean Electrical Power (IEEE) (2009) 376.
- [19] F. Rafik, H. Gualous, R. Gallay, A. Crausaz, A. Berthon, Frequency, thermal and voltage supercapacitor characterization and modeling, *Journal of Power Sources* 165 (2007) 928.
- [20] Z. Cheng, W. Chen, Q. Li, Z. Jiang, Z. Yang, Asia Pacific Power and Energy Engineering Conference (IEEE) (2010) 1.
- [21] 2008 IEEE Power and Energy Society General Meeting Conversion and Delivery of Electrical Energy in the 21st Century (IEEE), 1–7 (2008).
- [22] A.S. Weddell, G.V. Merrett, T.J. Kazmierski, B.M. Al-Hashimi, Accurate supercapacitor modeling for energy harvesting wireless sensor nodes, *IEEE Transaction on Circuits and Systems. II: Express Briefs* 58 (2011) 911.
- [23] P. Bjornbom, Charge/discharge of an electrochemical supercapacitor electrode pore; non-uniqueness of mathematical models, *Electrochemistry Communications* 9 (2007) 211.
- [24] K. Tsay, L. Zhang, J. Zhang, Effects of electrode layer composition/thickness and electrolyte concentration on both specific capacitance and energy density of supercapacitor, *Electrochimica Acta* 60 (2012) 428.